



Porter, R. (2019). An extended linear shallow water equation. *Journal of Fluid Mechanics*, 413-427. <https://doi.org/10.1017/jfm.2019.555>

Peer reviewed version

License (if available):
Other

Link to published version (if available):
[10.1017/jfm.2019.555](https://doi.org/10.1017/jfm.2019.555)

[Link to publication record in Explore Bristol Research](#)
PDF-document

This is the accepted author manuscript (AAM). The final published version (version of record) is available online via Cambridge University Press at <https://doi.org/10.1017/jfm.2019.555> . Please refer to any applicable terms of use of the publisher.

University of Bristol - Explore Bristol Research

General rights

This document is made available in accordance with publisher policies. Please cite only the published version using the reference above. Full terms of use are available:
<http://www.bristol.ac.uk/red/research-policy/pure/user-guides/ebr-terms/>

An extended linear shallow water equation

By **R. PORTER**

School of Mathematics, University of Bristol, Bristol, BS8 1TW, UK

(Received 4 July 2019)

An extension to the classical shallow water equation (SWE) is derived which exactly satisfies the bed condition and can be regarded as an approximation to wave scattering at the next order in the small parameter $(h/\lambda)^2$ (depth to wavelength ratio squared.) In the frequency domain, the extended SWE shares the same simple structure as the standard SWE with coefficients modified by terms relating to the bed variation. In three dimensions the governing equation demonstrates that variable topography gives rise to anisotropic effects on wave scattering not present in the standard SWE with consequences for the design of water wave metamaterials. Numerical examples illustrate that approximations to wave scattering using the extended SWE are significantly improved in comparison with the standard SWE.

1. Introduction

The linearised Shallow Water Equation (SWE) is used to describe the propagation of surface gravity waves over variable bathymetry $z = -h(x, y)$ in the long wavelength limit, $\lambda \gg h$, and is commonly expressed (e.g. Lamb (1932), Stoker (1957), Whitham (1974)) in the form

$$g\nabla \cdot (h\nabla\zeta) = \zeta_{tt} \quad (1.1)$$

where g is acceleration due to gravity, $\nabla = (\partial_x, \partial_y)$ and $\zeta(x, y, t)$ is the free surface elevation assumed to be small in the sense that $|\nabla\zeta| \sim |\zeta|/\lambda \ll (h/\lambda)^3$. This latter assumption justifies the linearisation of the governing equations in what follows; see Ursell (1953) or Mei & Le Méhauté (1966).

When time-harmonic motion is considered and $\zeta(x, y, t) = \Re\{\eta(x, y)e^{-i\omega t}\}$, (1.1) is transformed to

$$\nabla \cdot (h\nabla\eta) + K\eta = 0 \quad (1.2)$$

where $K = \omega^2/g$. Assuming that the local wavenumber $k(x, y) = 2\pi/\lambda$ is determined by the local depth $h(x, y)$ as though the bed were flat we have $k^2h = K$ and this corresponds to the long-wavelength ($kh \rightarrow 0$) limit of the exact water wave dispersion relation $k \tanh kh = K$. Under the SWE waves are non-dispersive.

The SWE is practically limited to the study of very long waves such as tidal modelling or tsunami wave simulation. For coastal wave dynamics, modern computations are normally based on higher-order long-wavelength models which incorporate weakly dispersive and nonlinear effects. These tend to be classified as Boussinesq-type models (see e.g. Brocchini (2013)). Recently the SWE has received renewed attention because of its structural similarity to 2nd order partial differential equations describing waves in acoustics and electromagnetics and this analogue has seen it used as a model for producing exotic effects in water wave scattering such as invisibility cloaking, negative refraction, wave-shifting and other wave control mechanisms (see, e.g., Farhat *et al.* (2008), Chen

et al. (2009), Farhat *et al.* (2010), Hu *et al.* (2011), Berraquero *et al.* (2013), Wang *et al.* (2015), Dupont *et al.* (2015), Maurel *et al.* (2017).) Some of these studies include experimental results (see, for example, Farhat *et al.* (2008), Berraquero *et al.* (2015)) in which good agreement with shallow water theory is not always clear cut – understandable not least because the conditions of shallow water theory are not easily met.

In the classical derivation of (1.1) the velocity and pressure fields along with the free surface elevation are non-dimensionalised before being expanded in the small parameter $\mu^2 = (H/L)^2$ in terms of characteristic depth and horizontal lengthscales, H and L , which are substituted into the governing mass and momentum equations (see, for example, Stoker (1957), Friedrichs (1948)). At leading order the vertical acceleration is neglected and, as a consequence, the flow velocity is expressed as $\mathbf{u}(x, y, z, t) = u(x, y, t)\hat{\mathbf{x}} + v(x, y, t)\hat{\mathbf{y}} + w(x, y, z, t)\hat{\mathbf{z}}$ and it quickly follows that the governing equation (1.1) results. Continuity implies that the leading order vertical velocity possesses a linear profile in z , the depth coordinate, detail which is not required in first-order models but which is used when the governing equations are expanded to next order in μ^2 . This expansion to higher-order in μ^2 lies at the heart of Boussinesq models and the process above is described in Peregrine (1967) (see also Madsen *et al.* (1991) Brocchini (2013)). Presumably in pursuit of governing equations which capture typical effects observed in shallow coastal waters, such accounts include nonlinearity by assuming an Ursell number of $O(1)$; see Ursell (1953). It is less common to find studies based on the linearised Boussinesq equations although exceptions exist; see for example Cho *et al.* (2007).

The main purpose of the present paper is to consider the extension of the linearised shallow water equations to second order in μ^2 (i.e. coinciding with the linearised Boussinesq equations) and demonstrate how it is possible to transform the frequency-domain versions of those equations back into the form of (1.2). There are several reasons for wanting to do this. The first is that we expect both improved accuracy and an extension of the range of values of h/λ over which the SWE can reliably operate. The second is to provide an explanation for long-wavelength limit of the so-called Complementary Mild-Slope Equation, considered recently by Porter (2019). The third is that the extended SWE will be shown to possess a structure similar to (1.2) and therefore can be implemented within existing computational schemes with minimal cost. The final reason is that the modified equations in a three-dimensional setting will be shown to demonstrate anisotropy in wave speeds over variable bathymetry. Specifically local wave speeds depend on the wave heading in a manner explicitly related to $h(x, y)$. This could be particularly significant in application areas referred to earlier in which wave control, designed using the transformation media approach, requires anisotropic effects to be embedded in a SWE. This has previously been achieved by introducing water wave metamaterials – microstructures which mimic this anisotropy under a multiple scales/homogenisation approach.

The starting point for this paper could have been a linearised version of the equations of Peregrine (1967) there are benefits to deriving the basis of the extended SWE afresh. This allows us to remove the complication of scaling, expressed clearly, for example, in the recent account of Duran *et al.* (2018) and assume from the outset the velocity fields which apply at second order. It provides the reader with a clear quick derivation of the equations which are subsequently under consideration and allows intermediate points in the derivation to be discussed.

In addition to the Boussinesq model already mentioned, there are a wealth of shallow water wave models which are designed to incorporate a variety of different effects from fully to weakly non-linear to non-dispersive or weakly-dispersive as well as bathymetric effects. Many of the weakly-dispersive models, when linearised, coincide with the linearised Boussinesq equations and hence those that form the basis of the extended SWE

here. This includes, for example, the linearised Green & Nagdhi (1976) equations which themselves are a particular version of the Serre equations (see, e.g. Dias & Milewski (2010)).

The development of the extended SWE is easiest to demonstrate in two dimensions and we consider this next, before extending ideas to the three-dimensional problem in §3. In §4 the extended SWE is tested against the standard SWE in two examples by comparing with results from solving the unapproximated full linear equations. Some attention is paid to bathymetry with sharp corners and one surprising outcome of the analysis is that the extended SWE model predicts discontinuities in the free surface elevation above discontinuities in h .

2. Formulation: two dimensions

The flow velocity is written $\mathbf{u} = (u(x, z, t), 0, w(x, z, t))$ and, adopting the standard assumptions of shallow water theory (see Stoker (1957) for example) we make the leading order approximation that

$$u(x, z, t) \approx U(x, t) \quad (2.1)$$

and

$$w(x, z, t) \approx (z/h(x) + 1)\zeta_t(x, t) + (zh'(x)/h(x))U(x, t). \quad (2.2)$$

This choice of w ensures that the kinematic (no-flow) condition on the bed $z = -h(x)$, expressed by

$$h'(x)u(x, -h(x), t) + w(x, -h(x), t) = 0 \quad (2.3)$$

is satisfied exactly. On the surface $z = \zeta(x, t)$ the linearised kinematic condition

$$w(x, 0, t) = \zeta_t(x, t) \quad (2.4)$$

holds. The linear profile (2.2) is anticipated by Stoker (1957) and adopted by Peregrine (1967).

We apply continuity $u_x + w_z = 0$ in a depth-averaged sense of

$$[w(x, z, t)]_{-h(x)}^0 = - \int_{-h(x)}^0 u_x(x, z, t) dz. \quad (2.5)$$

After substitution from (2.1) and use of the kinematic equations on the bed and the surface, (2.3), (2.4), we arrive at

$$\zeta_t = -(hU)_x. \quad (2.6)$$

a result which does not require the definition of w as expressed in (2.2). In passing, we note that the use of (2.6) in (2.2) results in a simplified version of (2.2) namely

$$w \approx \zeta_t - zU_x \quad (2.7)$$

which is less intuitive than the form originally adopted, although it is clearer to see from (2.7) that $u_x + w_z = 0$ is satisfied pointwise throughout the fluid.

The vertical component of the (linearised) momentum equation is

$$\rho w_t = -p_z - \rho g, \quad -h(x) < z < 0 \quad (2.8)$$

where ρ is the fluid density and $p(x, z, t)$ is the pressure. In the derivation of the standard SWE the term ρw_t does not contribute at leading order and is therefore neglected. Following arguments given in the Introduction we retain the ρw_t term and, after using

(2.2) in (2.8), we find

$$p_z = -\rho g - \rho(z/h(x) + 1)\zeta_{tt} - \rho(zh'(x)/h(x))U_t \quad (2.9)$$

(we could use (2.7) in place of (2.2), but there is no significant algebraic benefit in what follows.) Integrating (to leading order) and enforcing $p = p_a$, atmospheric pressure, on $z = \zeta(x, t)$ gives

$$p(x, z, t) = p_a + \rho g(\zeta - z) - \rho \left(\frac{z^2}{2h(x)} + z \right) \zeta_{tt} - \rho \frac{z^2 h'(x)}{2h(x)} U_t. \quad (2.10)$$

This expression will now be used in the horizontal component of the momentum equation which, like the continuity equation, is applied in a vertically-averaged sense. Thus

$$\begin{aligned} Q_t &= -\frac{1}{\rho} \int_{-h(x)}^0 p_x dz \\ &= -gh\zeta_x - \frac{1}{3}h^2\zeta_{ttx} - \frac{1}{6}hh'\zeta_{tt} + \frac{1}{6}h^2h'U_{tx} + \frac{1}{6}(h^2h'' - hh'^2)U_t \end{aligned} \quad (2.11)$$

expressed in terms of $Q(x, t)$, the depth-averaged horizontal flux and includes contributions beyond leading order terms in the expansion in the bed shallowness parameter on the left-hand side of but can be made equal to its leading order value $hU(x, t)$ elsewhere. Henceforth the dependence of h upon x is dropped for clarity. The relation $hU_{tx} = (hU_t)_x - h'U_t$ is used to express, via (2.6), the above in the form

$$\left\{ 1 + \frac{1}{3}h'^2 - \frac{1}{6}hh'' \right\} Q_t = -gh\zeta_x - \frac{1}{3}h^2\zeta_{ttx} - \frac{1}{3}hh'\zeta_{tt}. \quad (2.12)$$

Dividing by the bracketed term on the left-hand side and differentiating with respect to x allows us to eliminate Q using (2.6) to obtain

$$\zeta_{tt} = \frac{\partial}{\partial x} \left(\frac{h(g\zeta + \frac{1}{3}h\zeta_{tt})_x}{1 + \frac{1}{3}h'^2 - \frac{1}{6}hh''} \right) \quad (2.13)$$

and this is the time-dependent extended SWE though not exactly aligned to the form expressed in (1.1). Assuming a time-harmonic dependence by writing $\zeta(x, t) = \Re\{\eta(x)e^{-i\omega t}\}$ results in

$$\left(\frac{h((1 - \frac{1}{3}Kh)\eta)'}{1 + \frac{1}{3}h'^2 - \frac{1}{6}hh''} \right)' + K\eta = 0 \quad (2.14)$$

where $K = \omega^2/g$ and writing $\psi(x) = (1 - \frac{1}{3}Kh(x))\eta(x)$ allows us to express the SWE in the same form as the original version (1.2), as

$$(\hat{h}\psi)' + \hat{K}\psi = 0 \quad (2.15)$$

where

$$\begin{aligned} \hat{h}(x) &= h(x)/(1 + \frac{1}{3}h'^2(x) - \frac{1}{6}h(x)h''(x)), \\ \hat{K}(x) &= K/(1 - \frac{1}{3}Kh(x)) \end{aligned} \quad (2.16)$$

are scaled versions of h and K .

Instead of eliminating Q in favour of η we can return to (2.12), differentiate with respect to t and use (2.6) to find that

$$\left\{ 1 + \frac{1}{3}h'^2 - \frac{1}{6}hh'' \right\} Q_{tt} = h(gQ_x + \frac{1}{3}hQ_{ttx})_x, \quad (2.17)$$

with $\zeta_t = -Q_x$, is an alternative to (2.13). If $Q(x, t) = \Re\{q(x)e^{-i\omega t}\}$ then (2.17) reduces to

$$(\hat{K}^{-1}q')' + \hat{h}^{-1}q = 0, \quad (2.18)$$

with $\eta = -(i/\omega)q'$, which becomes an alternative to (2.15) which retains the structure of (1.2).

Whilst (2.15) and (2.18) provide equally valid descriptions of wave scattering by the bed, $h(x)$, the latter version is able cope with discontinuities in bed slopes since we can use the differential equation to determine the jump condition

$$[q'(x)]_{c-}^{c+} = \frac{1}{6}\hat{K}(c)q(c)[h'(x)]_{c-}^{c+} \quad (2.19)$$

where $x = c$ is a point of discontinuity in $h'(x)$. The relationship between q and the surface elevation implies that $\eta(x)$ is discontinuous whenever $h'(x)$ is. This seems odd but is simply an outcome of the underlying assumptions adopted in this approximation. We remark that, in the standard SWE, $\eta'(x)$ is discontinuous at corners in the bed for similar reasons.

A transformed version of the SWE (2.18) can be developed by introducing the scaling

$$q(x) = \varphi(x)/\sqrt{1 - \frac{1}{3}Kh} \quad (2.20)$$

which, after substituting into (2.18) and working through the algebra, results in

$$\varphi''(x) + \{\hat{K}(1 + \frac{1}{3}v(h)h'^2)/h\}\varphi(x) = 0 \quad (2.21)$$

where $v(h) = 1 + \frac{1}{12}\hat{K}h \approx 1$ for $Kh \ll 1$. This form of the SWE does not contain terms proportional to $h''(x)$ and thus $\varphi(x)$ is continuous even when h' is discontinuous. The free surface is reconstructed in terms of $\varphi(x)$ with

$$\eta(x) = \frac{(-i/\omega)}{\sqrt{1 - \frac{1}{3}Kh}}(\varphi'(x) + \frac{1}{6}\hat{K}h'\varphi(x)) \quad (2.22)$$

and discontinuities in $\eta(x)$ at points of discontinuity of $h'(x)$ are now clearly manifested by the second term. If we further let $\Omega(x) = \varphi'(x)$, then (2.21) implies that $\Omega'(x) = -\{\hat{K}(1 + \frac{1}{3}v(h)h'^2)/h\}\varphi(x)$ and it follows that

$$(\hat{h}\Omega')' + K\Omega = 0 \quad (2.23)$$

where

$$\hat{h}(x) = h(x)\frac{(1 - \frac{1}{3}Kh(x))}{(1 + \frac{1}{3}v(h)h'^2(x))} \quad (2.24)$$

is once more aligned with (1.2) and becomes the alternative to (2.15) without discontinuities in the dependent variable at points of discontinuity in the bed. The transformed version of (2.22) is

$$\eta(x) = \frac{(-i/\omega)}{\sqrt{1 - \frac{1}{3}Kh}}\left(\Omega(x) - \frac{\frac{1}{6}hh'}{1 + \frac{1}{3}v(h)h'^2}\Omega'(x)\right). \quad (2.25)$$

In practice $\hat{h}(x)$ as defined by (2.24) can be used in place of $h(x)$ in (1.2) to furnish results for the extended SWE for all continuous $h(x)$.

For waves propagating over a flat bed, $h(x) = h_0$ a constant, say, any one of (2.15), (2.18), (2.21) or (2.23) can be used to show that solutions are given by $\eta(x) = e^{\pm ik_0 x}$ where k_0 satisfies $k_0^2 h_0^2 = Kh_0/(1 - \frac{1}{3}Kh_0)$. This agrees to second order in Kh_0 with the expansion of the exact dispersion relation for waves over constant depth h_0 , namely $K = k_0 \tanh k_0 h_0$ which is readily found to be $k_0^2 h_0^2 \approx Kh_0(1 + \frac{1}{3}Kh_0 + O(Kh_0)^2)$ for $Kh_0 \ll 1$. In contrast, solutions of (1.2) are given in terms of a wavenumber satisfying

$k_0^2 h_0^2 = K h_0$, which only captures the leading order behaviour. Thus, the extended SWE includes weak dispersion not captured within the original SWE.

Porter (2019) has independently derived a version of (2.21) which agrees at leading order in the bed slope h' and its three-dimensional analogue seen later in (3.18) but with $\hat{K} = K$, $v(h) = 1$ by considering the long-wavelength limit of the Complementary Mild-Slope Equation, originally due to Kim & Bai (2004) and Toledo & Agnon (2010).

The long wavelength limit of Porter (2019) fails to capture the factors $1 - \frac{1}{3}Kh$ responsible for the weakly-dispersive effect in (2.21), (2.22) nor the lower-order corrective term $v(h)$. It is supposed that this mismatch is a consequence of the fundamentally different initial starting points that have been adopted in the modelling, Porter's (2019) derivation evolving from a variational formulation of the problem.

We also note the relationship of the equations we have derived to the work of Ehrenmark (2005) who considered the effect of wave propagation over a constant plane slope on the local dispersion relation. In that work a modified dispersion relation was proposed which replaced the local depth $h(x)$ by an effective depth $h(x)/(1 + \frac{1}{3}h'^2(x) + O(h'^4))$ which agrees at leading order with both the definition of $\hat{h}(x)$ in (2.16) and of $\hat{\hat{h}}(x)$ in (2.24).

3. Three dimensions

Now the bed is given by $z = -h(x, y)$ and the free surface by $z = \zeta(x, y, t)$. One can easily show that the analogue of the continuity equation (2.6) is

$$\zeta_t = -\nabla \cdot (h\mathbf{U}) \quad (3.1)$$

where $\mathbf{U} = (U(x, y, t), V(x, y, t))$, $\nabla = (\partial_x, \partial_y)$ following an assumption that the flow velocity takes the form

$$\mathbf{u} \approx (\mathbf{U}, (z/h + 1)\zeta_t + (z/h)\nabla h \cdot \mathbf{U}) \quad (3.2)$$

and satisfies $w = \zeta_t$ on $z = 0$ and $w + \nabla h \cdot \mathbf{U} = 0$ on $z = -h(x, y)$.

Following the derivation in §2, with the momentum equation in the horizontal plane written $\rho\mathbf{U}_t = -\nabla p$ leads to the equation for the depth-integrated flux \mathbf{Q} (equal to $h\mathbf{U}$ at leading order)

$$\mathbf{Q}_t = -gh\nabla\zeta - \frac{1}{3}h^2\nabla\zeta_{tt} - \frac{1}{6}h\{\zeta_{tt} + (\nabla h \cdot (\mathbf{Q}_t/h))\}\nabla h + \frac{1}{6}h^2\nabla(\nabla h \cdot (\mathbf{Q}_t/h)) \quad (3.3)$$

and this can be arranged in the form

$$\mathbf{Q}_t = -gh\nabla\zeta - \frac{1}{3}h^2\nabla\zeta_{tt} - \frac{h\zeta_{tt}}{6}\nabla h - \frac{1}{3}h(\nabla h \cdot (\mathbf{Q}_t/h))\nabla h + \frac{1}{6}h\nabla(\nabla h \cdot \mathbf{Q}_t). \quad (3.4)$$

With some more work, this equation can be reduced to

$$\mathbf{Q}_t + \frac{1}{3}(\nabla h \cdot \mathbf{Q}_t)\nabla h - \frac{1}{6}h\mathbf{h}''\mathbf{Q}_t + \frac{1}{6}h\mathbf{D}\mathbf{Q}_t = -\nabla(g\zeta + \frac{1}{3}h\zeta_{tt}) \quad (3.5)$$

where \mathbf{h}'' represents the 2×2 Hessian matrix of $h(x, y)$ which multiplies vector \mathbf{Q}_t and

$$\mathbf{D} = \begin{pmatrix} 0 & \mathbf{t} \cdot \nabla \\ -\mathbf{t} \cdot \nabla & 0 \end{pmatrix} \quad (3.6)$$

is an antisymmetric differential operator where $\mathbf{t} = (-h_y, h_x)$ is directed along level curves of $h(x, y)$.

Introducing \mathbf{I} as the 2×2 Identity matrix and writing

$$\mathbf{h}'^2 = (\nabla h)(\nabla h)^T = \begin{pmatrix} h_x^2 & h_x h_y \\ h_x h_y & h_y^2 \end{pmatrix} \quad (3.7)$$

– notation aligned to the two-dimensional setting – we may arrange (3.6) as

$$\{I + \frac{1}{3}h'^2 - \frac{1}{6}hh'' + \frac{1}{6}hD\}\mathbf{Q}_t = -h\nabla(g\zeta + \frac{1}{3}h\zeta_{tt}). \quad (3.8)$$

As it stands we are not able to make eliminate \mathbf{Q} in favour of ζ as we did in the two-dimensional case. If we decide to eliminate ζ in favour of \mathbf{Q} by taking the time derivative of (3.8) and substituting from (3.1) we find

$$h^{-1}\{I + \frac{1}{3}h'^2 - \frac{1}{6}hh'' + \frac{1}{6}hD\}\mathbf{Q}_{tt} = \nabla(g\nabla \cdot \mathbf{Q} + \frac{1}{3}h\nabla \cdot \mathbf{Q}_{tt}) \quad (3.9)$$

where $\zeta_t = -\nabla \cdot \mathbf{Q}$. Thus, in the time domain, it appears that we can do no better than the vector governing equation (3.9). With $\mathbf{Q}(x, y, t) = \Re\{\mathbf{q}(x, y)e^{-i\omega t}\}$ we have

$$\nabla(\hat{K}^{-1}\nabla \cdot \mathbf{q}) + h^{-1}\{I + \frac{1}{3}h'^2 - \frac{1}{6}hh'' + \frac{1}{6}hD\}\mathbf{q} = 0 \quad (3.10)$$

with $\eta(x, y) = -(i/\omega)\nabla \cdot \mathbf{q}$ and

$$\hat{K}(x, y) = K/(1 - \frac{1}{3}Kh(x, y)) \quad (3.11)$$

is the extension of (2.16) to functions of two variables.

Consider that the bed $h(x, y)$ has a discontinuity in gradients at points \mathbf{c} along the curve $\Gamma \in \mathbb{R}^2$ having unit normal $\hat{\mathbf{n}}$ directed from Γ^- to Γ^+ . Then (3.10) shows that the jump conditions for points \mathbf{c} on Γ take the form

$$[\nabla \cdot \mathbf{q}]_{\Gamma^-}^{\Gamma^+} = \frac{1}{6}\hat{K}(\mathbf{c})\hat{\mathbf{n}} \cdot \mathbf{q}(\mathbf{c}) [\hat{\mathbf{n}} \cdot \nabla h]_{\Gamma^-}^{\Gamma^+}. \quad (3.12)$$

Thus far, the three-dimensional case has failed to furnish a scalar equation either in time or frequency domains and the vector equations for \mathbf{Q} and \mathbf{q} are complicated by the appearance of the operator D , not present in the two-dimensional case.

However, as in the two-dimensional case, we can make further useful progress by introducing the scaling

$$\mathbf{q}(x, y) = \boldsymbol{\varphi}(x, y)/\sqrt{1 - \frac{1}{3}Kh} \quad (3.13)$$

into (3.10). After considerable, but routine, algebra we arrive at

$$\nabla(\nabla \cdot \boldsymbol{\varphi}) + (\hat{K}/h)\{I + \frac{1}{3}v(h)h'^2\}\boldsymbol{\varphi} = 0 \quad (3.14)$$

and $v(h) = 1 + \frac{1}{12}\hat{K}h$ is the same factor as derived in the previous section. Now the function $\boldsymbol{\varphi}(x, y)$ is continuous even at discontinuities in the gradients of the bed. The free surface is found to be related to $\boldsymbol{\varphi}$ by

$$\eta(x, y) = \frac{(-i/\omega)}{\sqrt{1 - \frac{1}{3}Kh}} \left(\nabla \cdot \boldsymbol{\varphi} + \frac{1}{6}\hat{K}\nabla h \cdot \boldsymbol{\varphi} \right). \quad (3.15)$$

The simplified vector equation (3.14) also provides the platform for a scalar version of the extended SWE in three dimensions since writing $\Omega(x, y) = \nabla \cdot \boldsymbol{\varphi}$ means that (3.14) becomes

$$\boldsymbol{\varphi} = -(\hat{h}/K)\nabla\Omega \quad (3.16)$$

where

$$\begin{aligned} \hat{h}(x, y) &= h(x, y)(1 - \frac{1}{3}Kh)(I + \frac{1}{3}v(h)h'^2)^{-1} \\ &= h(x, y)(1 - \frac{1}{3}Kh) \left(I - \frac{v(h)}{(3 + v(h)|\nabla h|^2)}h'^2 \right). \end{aligned} \quad (3.17)$$

Thus, we arrive at

$$\nabla \cdot (\hat{h}\nabla\Omega) + K\Omega = 0 \quad (3.18)$$

as the scalar version of the extended SWE for $\Omega(x, y)$ presented in the form (1.2) but with the scalar function $h(x, y)$ replaced by the 2×2 matrix $\hat{\mathbf{h}}(x, y)$. The surface elevation is reconstructed from Ω using

$$\eta(x, y) = \frac{(-i/\omega)}{\sqrt{1 - \frac{1}{3}Kh}} \left(\Omega - \frac{1}{6}h\nabla h \cdot \left((1 + \frac{1}{3}v(h)h'^2)^{-1} \nabla \Omega \right) \right) \quad (3.19)$$

where discontinuities in ∇h can be seen to produce corresponding discontinuities in η .

The development from \mathbf{q} through to Ω follows closely the work of Toledo & Agnon (2010) (the variable Ω is used in recognition of this) who developed a scalar Complementary Mild-Slope Equation (CMSE) from the original vector equation derived by Kim & Bai (2004). The CMSE, given in (A 2), is a depth-averaged model in which the depth variation in the fluid is approximated in such a way to satisfy the bed condition exactly and formally requires shallow bed gradients but is not restricted to long wavelengths. The result of taking the limit $Kh \rightarrow 0$ in Toledo & Agnon (2010)'s scalar equation is (A 3) which coincides with (3.18) provided approximations to leading order in Kh are made to $\hat{K} \approx K$ and $v(h) \approx 1$. In other words there are differences between (A 3) and (3.18) in higher order terms in Kh . This limit is also noted by Porter (2019), who derived the same scalar Complementary Mild-Slope Equation but using a more general variational principle to that used by Kim & Bai (2004).

Both the scalar equation (3.18) and the vector equation (3.14) representing three-dimensional scattering demonstrate anisotropy. That is, waves taken to propagate in different directions at the same point (x, y) in space will, in general, travel with different speeds relating to the gradients of the bed in those directions. This might come as a surprise to some readers but is possibly known to others not least since it can be inferred from Toledo & Agnon (2010)'s work. What *is* most certainly useful is the explicit dependence of those wave speeds on the function $h(x, y)$ which can be inferred from (3.17). Indeed, the real benefit of using the extended SWE in place of the CMSE is the simple explicit dependence on h in the former compared to the complex implicit dependence on h in the latter – see (A 2).

4. Examples

4.1. Numerical solutions: two-dimensional wave scattering

In the case of reflection and transmission of waves of frequency ω incident from $x = -\infty$ over a finite region of variable two-dimensional bathymetry between two flat semi-infinite sections, numerical solutions of any of the versions of the SWE derived in §2 are easy to compute. We shall outline the method applied to the version given by (2.23) for the variable $\Omega(x)$ which does not require special treatment at discontinuities in the bed. Assume that for $x < 0$, $h(x) = h_0$ and for $x > L$, $h(x) = h_L$ and the $h(x)$ is smooth. Then in $x < 0$

$$\Omega(x) = e^{ik_0x} + R e^{-ik_0x} \quad (4.1)$$

and in $x > L$

$$\Omega(x) = T e^{ik_Lx} \quad (4.2)$$

where $k_0 h_0 = \sqrt{Kh_0/(1 - \frac{1}{3}Kh_0)}$ and $k_L h_L = \sqrt{Kh_L/(1 - \frac{1}{3}Kh_L)}$ and R, T represent reflection and transmission coefficients. In $0 < x < L$ the solution is determined by (2.23). Matching solutions across the two boundaries and elementary manipulation of

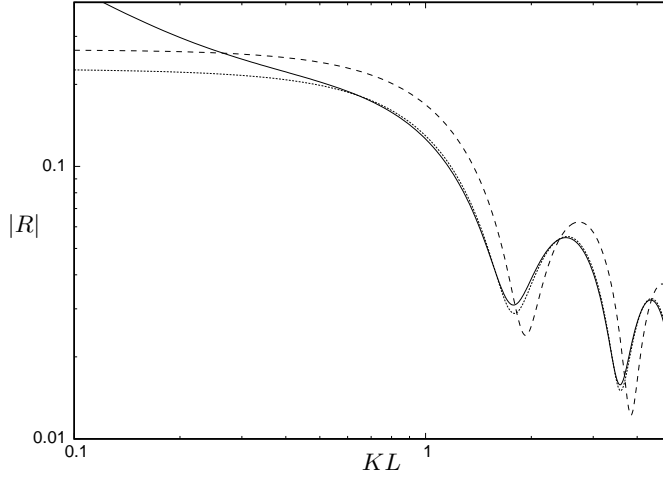


FIGURE 1. Modulus of reflection coefficient against KL at $Kh_0 = 0.6$, $h_L/h_0 = \frac{1}{3}$ (the Booij problem): full linear theory (dotted), standard SWE (dashed), extended SWE (solid).

the algebra that results shows us that R and T can be obtained from

$$\begin{pmatrix} R \\ T \end{pmatrix} = \begin{pmatrix} i(K/k_0)p_2(1) - p_1(1) & e^{ik_L L} \\ i(K/k_0)q_2(1) - q_1(1) & i(K/k_L)e^{ik_L L} \end{pmatrix}^{-1} \begin{pmatrix} i(K/k_0)p_2(1) + p_1(1) \\ i(K/k_0)q_2(1) + q_1(1) \end{pmatrix} \quad (4.3)$$

where $p_i(1)$, $q_i(1)$ are determined from solving the coupled first-order differential equations

$$p'_i(\xi) = Lq_i(\xi)/\hat{h}(L\xi), \quad q'_i(\xi) = -KLp_i(\xi) \quad 0 < \xi < 1 \quad (4.4)$$

for $i = 1, 2$ subject to initial conditions $p_1(0) = 1$, $q_1(0) = 0$, $p_2(0) = 0$, $q_2(0) = 1$. On account of the scaling used to define the free surface in (2.25), the transmission coefficient associated with free surface amplitudes requires scaling by the factor $\sqrt{1 - \frac{1}{3}Kh_L}/\sqrt{1 - \frac{1}{3}Kh_0}$.

The standard SWE uses the same scheme but with \hat{h} replaced by h and the definition of k_0 and k_L replaced by $k_0 = \sqrt{K/h_0}$ and $k_L = \sqrt{K/h_L}$. The additional scaling of the transmission coefficient referred to above is not necessary.

4.2. The Booij problem

For historical reasons the Booij problem (Booij (1983)) has become a standard test case for assessing two-dimensional scattering approximations. A linear slope connects the depth h_0 to h_L over $0 < x < L$ and the particular set of results Booij generated are taken for $h_L/h_0 = \frac{1}{3}$, $Kh_0 = 0.6$ and $|R|$ is plotted as a function of KL . Since Kh_0 is fixed and not especially small and the horizontal axis effectively measures steepness of slope, this is not such an enlightening test of the SWE. Indeed, we see in Fig. 1 that the extended SWE fails compared to the exact results as $KL \rightarrow 0$ and the slope approaches vertical. Neither the standard nor the extended SWE is designed to operate in this regime and it is simply good fortune that the standard SWE stands as an acceptable approximation up to the point of a vertical step. Instead, the extended SWE fails due to the presence of the h'^2 in the denominator of \hat{h} or \hat{h} which drives the ‘effective depth’ to zero as $KL \rightarrow 0$ and hence the reflection coefficient tends to unity. For smaller gradients (larger values of KL) below 45° Fig. 1 shows that the extended SWE outperforms the standard

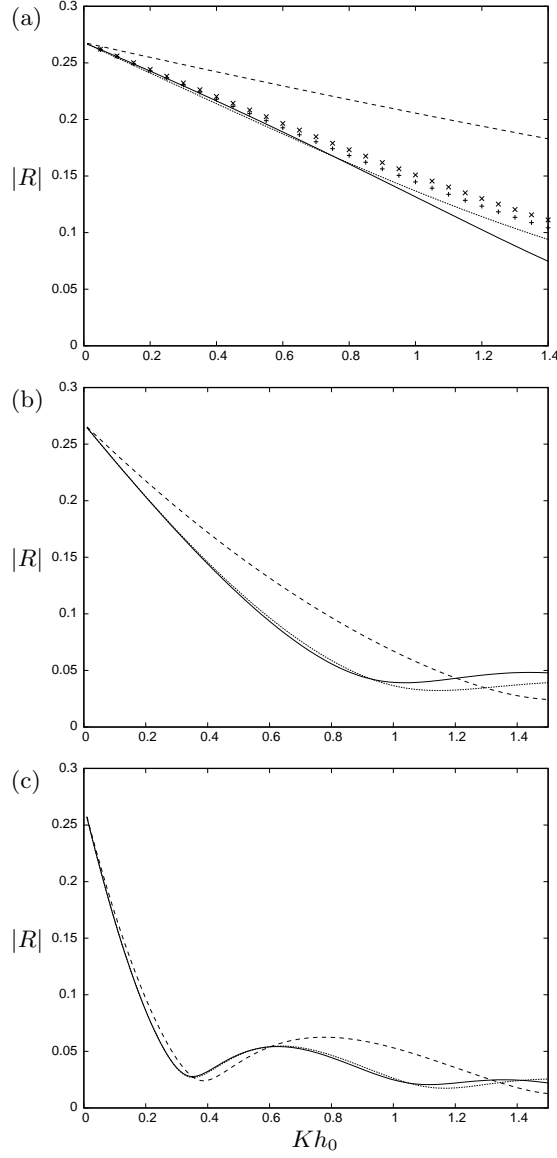


FIGURE 2. Modulus of reflection coefficient against Kh_0 for a linear ramp with $h_L/h_0 = \frac{1}{3}$ and $h_0/L = 1, \frac{1}{2}, \frac{1}{4}$ in (a),(b),(c): full linear theory (dotted), standard SWE (dashed), extended SWE (solid). In (a) + are results from the CMSE, \times results from the MMSEs.

SWE by a significant margin and results are in excellent agreement with the accurate computations based on full linear theory (using the method of Porter & Porter (2000)). Fig. 1 is very similar both qualitatively and quantitatively to Fig. 8 of Ehrenmark (2005) and the explanation for this is connected to the discussion at the end of §2.

More informative results are shown in Figs. 2. These are again for a linear slope, but the slope angle is fixed by fixing values of h_L/h_0 and h_0/L in each plot and the frequency of incident waves varies from the long wavelength limit $Kh_0 \rightarrow 0$ to shorter waves for increasing Kh_0 . There is a quite remarkable improvement both in the relative performance of the extended SWE over the standard version and in the range of values

of Kh_0 over which good agreement with the exact result is maintained. The standard SWE provides closer agreement for shallower gradients as might be expected and the extended SWE works well up to slopes close to 45° although the agreement falls away rapidly for steeper slopes (as Fig. 1 has already shown).

Fig. 2(a) also provides, for comparison, results obtained using the scalar CMSE and the MMSE, given in the Appendix. For values of $Kh_0 > 1.4$, the CMSE and MMSE become increasingly accurate whilst the extended SWE diverges from the exact results. The extended SWE is arguably the best fit to the exact results for $Kh < 1$. Similar conclusions can be drawn in Figs. 2(b,c) through data from CMSE and MMSE simulations have not been added to these plots as they are almost indistinguishable from the exact results over the range of values of Kh_0 plotted.

4.3. Roseau's solution

Roseau (1976) provides the only exact solution for waves propagating over a non-constant bathymetry. Thus we have

$$|R| = \left| \frac{\sinh[(k_0 h_0 - k_L h_L)/\beta]}{\sinh[(k_0 h_0 + k_L h_L)/\beta]} \right| \quad (4.5)$$

and $\beta \in (0, 1)$ is a shoaling parameter where the bed is given parametrically as $z(\xi) = -h(x(\xi))$ with

$$x(\xi)/h_0 = \xi - (2\pi\beta)^{-1}(1 - h_L/h_0) \ln(1 + e^{2\beta\pi\xi} + 2e^{\beta\pi\xi} \cos(\beta\pi)) \quad (4.6)$$

$$z(\xi)/h_0 = -1 + (\pi\beta)^{-1}(1 - h_L/h_0) \tan^{-1}\{\sin(\beta\pi)/(e^{-\beta\pi\xi} + \cos(\beta\pi))\}. \quad (4.7)$$

Then $h'(x(\xi)) = -z'(\xi)/x'(\xi)$ and $h''(x(\xi)) = -(z''(\xi)x'(\xi) - z'(\xi)x''(\xi))/(x'(\xi))^3$.

In Fig. 3 exact results computed from (4.5) where k_L and k_0 are defined by $K = k_L \tanh k_L h_L = k_0 \tanh k_0 h_0$ are compared with the new and standard SWE for a shoaling parameter $\beta = 0.5$ which gives a maximum gradient of 0.75 along the profile (see Porter & Porter (2006) for an illustration of the bed shape). The results demonstrate similar characteristics to those previously considered for the linear slope but without the oscillations due to multiple interference effects caused by the corners at the ends of the transition between the two depths.

Following Fig. 2(a) we have added results from the CMSE and the MMSE to Fig. 3 for comparison and we can draw similar conclusions here regarding the accuracy of the extended SWE compared to those models for sufficiently low values of Kh_0 .

5. Conclusions

We have extended the Shallow Water Equations (SWEs) to include the effect of the vertical acceleration of the fluid consistent with the the satisfaction of kinematic boundary conditions on the bed and the fluid surface. The new equations can be regarded as the approximation to the next order in the assumed small parameter $(h/\lambda)^2$. The resulting equation has the same structure in the frequency domain as the standard SWE, and includes a depth modified by bed gradients and dispersion modified by depth in a manner consistent with the leading order behaviour of the exact linear dispersion relation. In three dimensional scattering, the role of depth is replaced by a tensor-like term which is associated with anisotropy of phase speeds over variable bathymetry. This effect could potentially be exploited for wave control designed through the transformation media approach using normal bathymetric variations without the need for water wave metamaterials.

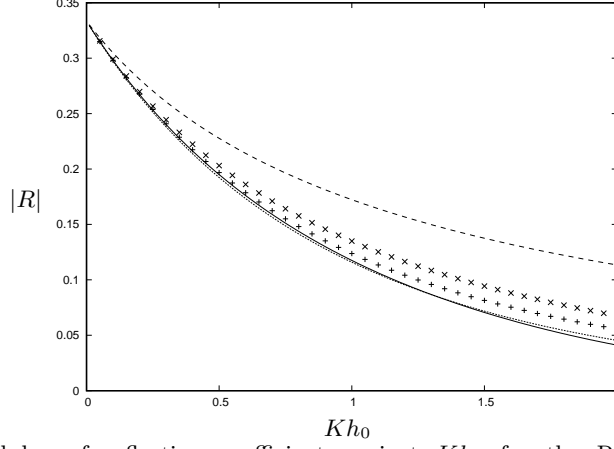


FIGURE 3. Modulus of reflection coefficient against Kh_0 for the Roseau problem with $h_L/h_0 = 0.25$, $\beta = 0.5$: full linear theory (dotted), standard SWE (dashed), extended SWE (solid). Also, + are results from the CMSE, \times results from the MMSEs.

Numerical examples have demonstrated that the extended SWE significant improvements compared to the standard SWE when compared against results computed using full linear theory and, provided bed gradients do not exceed 45° , good agreement is maintained over a large range of wavelengths. This suggests that the extended SWE can be employed as a versatile and accurate model of wave scattering for many practical applications.

The extended SWE coincides at leading order in Kh with the long-wavelength limit of Complementary Mild-Slope Equation (CMSE) of Kim & Bai (2004), Toledo & Agnon (2010) whilst the standard SWE is the long-wavelength limit of the Modified Mild-Slope Equations (see Appendix). This is not surprising in the sense that the former treats the bed condition exactly where the latter does not. The results obtained in this paper reinforces previous evidence that the CMSE is a superior depth-averaged model of wave scattering than the MMSE. Surprisingly, in the small sample of comparisons performed here, the extended SWE is shown to perform at least as well as, and arguably better, than both the CMSE and the MMSE for sufficiently long wavelength scattering problems.

Before drawing stronger conclusions further assessment of the extended SWE should be made, especially in fully three-dimensional scattering problems. However, a fair test will require accurate computations based on full linear theory and numerical software such as WAMIT (www.wamit.com) would be needed for this.

Appendix A

The Modified Mild Slope Equation (MMSE) in the form presented in Porter (2003) over the depth $h(x, y)$ is given as

$$\nabla \cdot (k^{-2} \nabla \varphi) + (1 - w(h) |\nabla h|^2) \varphi = 0 \quad (\text{A } 1)$$

for a function $\varphi(x, y)$ related to the free surface $\eta(x, y)$ where $k = k(h)$ satisfies $K = k \tanh kh$ and

$$w(h) = -\frac{\kappa^4 + 4\kappa^3 \sinh \kappa + 3\kappa^2 (\cosh 2\kappa + 2) - 3(2\kappa + \sinh \kappa)(\sinh 2\kappa - \sinh \kappa)}{3(\sinh \kappa + \kappa)^4}$$

where $\kappa = 2Kh$. Porter (2003) demonstrates that $w(h) \leq 0.030$ and that $w(h) \sim (Kh)^2/45$ as $Kh \rightarrow 0$ and $w(h) = O(e^{-2Kh})$ as $Kh \rightarrow \infty$. The long-wavelength limit of the MMSE is thus easily seen to be the SWE, (1.2). The Complementary Mild-Slope Equation (CMSE), as given in Toledo & Agnon (2010), and rederived in Porter (2019) is

$$\nabla \cdot \left(k^{-2} \left\{ \nabla \varphi - \frac{\gamma(h)}{1 + \gamma(h)|\nabla h|^2} (\nabla \varphi \cdot \nabla h) \nabla h \right\} \right) + \varphi = 0 \quad (\text{A } 2)$$

for a function $\varphi(x, y)$ related to the free surface $\eta(x, y)$ where

$$\gamma(h) = \frac{\kappa^4 + 4\kappa^3 \sinh \kappa + 3\kappa^2 (\cosh 2\kappa - 2) - 6\kappa \sinh \kappa + 3 \sinh \kappa (\sinh 2\kappa + \sinh \kappa)}{3(\sinh \kappa + \kappa)^4}.$$

It can be determined that $\gamma(h) \rightarrow \frac{1}{3}(1 - (4/15)(Kh)^2)$ as $Kh \rightarrow 0$ and so the long-wavelength limit of the CMSE is

$$\nabla \cdot \left(h \left\{ \nabla \varphi - \frac{1}{3 + |\nabla h|^2} (\nabla \varphi \cdot \nabla h) \nabla h \right\} \right) + K\varphi = 0. \quad (\text{A } 3)$$

REFERENCES

- BERRAQUERO, C. P., MAUREL, A., PETITJEANS, P. & PAGNEUX, V. (2013) Experimental realization of a water-wave metamaterial shifter. *Phys. Rev. E* **88**, 051002.
- BOOIJ, N. (1983) A note on the accuracy of the mild-slope equation. *Coastal Engng.* **7**, 191–203.
- BROCCINI, M. (2013) A reasoned overview on Boussinesq-type models: the interplay between physics, mathematics and numerics. *Proc. Roy. Soc. Lond. A* **469**, 20130496. <http://dx.doi.org/10.1098/rspa.2013.0496>
- CHEN, H., YANG, J., ZI, J. & CHAN, C. T. (2009) Transformation media for linear liquid surface waves. *EuroPhys. Lett.* **85**, 24004.
- CHO, H., Y-S, SOHN, D-H. & LEE, S. O. (2007) Practical modified scheme of linear shallow-water equations for distant propagation of tsunamis. *Ocean Eng.* **34**, 1769–1777.
- DIAS, F. & MILEWSKI, P. (2010) On the fully-nonlinear shallow-water generalized Serre equations *Phys. Lett. A* **374**, 1049–1053.
- DUPONT, G., KIMMOUN, O., MOLIN, B. GUENNEAU, S. & ENOCH, S. (2015) Numerical and experimental study of an invisibility carpet in a water channel. *Phys. Rev. E* **91**, 023010.
- DURAN, A., DUTYKH, D. & MITSOTAKIS, M. (2018) Peregrine’s system revisited. In *Nonlinear Waves and Pattern Dynamics*, Springer, doi.org/10.1007/978-3-319-78193-8
- EHRENMARK, U.T. (2005) An alternative dispersion relation for water waves over an inclined bed. *J. Fluid Mech.* **543**, 249–266.
- FARHAT, M., ENOCH, S., GUENNEAU, S. & MOVCHAN, A. (2008) Broadband cylindrical acoustic cloak for linear surface waves in a fluid. *Phys. Rev. Lett.* **101**, 134501.
- FARHAT, M., GUENNEAU, S., ENOCH, S. & MOVCHAN, A. (2010) All-angle-negative-refraction and ultra-refraction for liquid surface waves in 2D phononic crystals. *J. Comp. Appl. Math.* **234**(6), 2011–2019.
- FRIEDRICH, K.O. (1948) Water waves on a shallow sloping beach. *Comm. Pure Appl. Math.*, **1**, 109–134
- GREEN, A. & NAGHDI, P. (1976) A derivation of equations for wave propagation in water of variable depth *J. Fluid Mech.*, **78**, 237–246.
- HU, X., CHAN, C. T., HO, K.-M. & ZI, J. (2011) Negative effective gravity in water waves by periodic resonator arrays. *Phys. Rev. Lett.* **106**, 174501.
- KIM, J.W. & BAI, K.J. (2004) A new complementary mild-slope equation. *J. Fluid Mech.* **511**, 25–40.
- LAMB, H. (1932) *Hydrodynamics*. 6th Edition, Cambridge University Press.
- MADSEN, P.A., MURRAY, R. & SBRENSSEN, O.R. (1991) A new form of Boussinesq equations with improved linear dispersion characteristics. *Coastal Engng.* **15**, 371–388.
- MAUREL, A., MARIGO, J.-J., COBELLI, P., PETITJEANS, P. & PAGNEUX, V. (2017) Revisiting the anisotropy of metamaterials for water waves. *Phys. Rev. B* **96**, 134310.

- MEI, C.C. & LE MÉHAUTÉ (1966) Note on the equations of long waves over an uneven bottom. *J. Geophys. Res.* **71**(2), 393–400.
- MEI, C.C., STIASSNIE, M., & YU, D.K.-P. (2005) *Theory and Applications of Ocean Surface Waves Part 1: Linear Aspects*. World Scientific Publishing Co. Pte. Ltd.
- PEREGRINE, D.H. (1967) Long waves on a beach. *J. Fluid. Mech.* **27**, 815–827.
- PORTER, D. (2019) The Mild Slope Equations: A unified theory. *In preparation*.
- PORTER, R. & PORTER, D. (2000) Water wave scattering by a step of arbitrary profile. *J. Fluid. Mech.* **411**, 131–164.
- PORTER, D. (2003) The mild slope equations. *J. Fluid. Mech.* **494**, 51–63.
- PORTER, D. & PORTER, R. (2006) Approximations to water wave scattering by steep topography. *J. Fluid Mech.* **562**, 279–302.
- ROSEAU, M. (1976) *Asymptotic Wave Theory*, vol. 2 of North-Holland Series in Applied Mathematics and Mechanics. Amsterdam, The Netherlands.
- STOKER, J.J. (1957) *Water Waves*, Interscience, New York.
- TOLEDO, Y. & AGNON, Y. (2010) A scalar form of the complementary mild-slope equation. *J. Fluid Mech.* **656**, 407–416.
- URSELL, F. (1953) The long-wave paradox in the theory of gravity waves. *Proc. Camb. Phil. Soc.* **49**(4), 685–694.
- WANG, Z., ZHANG, P., NIE, X. & ZHANG, Y. (2015). Manipulating water wave propagation via gradient index media. *Sci. Rep.* **5**, 16846.
- WHITHAM, G.B. (1974) *Linear and Nonlinear Waves*. Wiley-interscience, New York.
- ZAREEI, A. & ALAM, M.-R. (2015). Cloaking in shallow-water waves via nonlinear medium transformation. *J. Fluid Mech.* **778**, 273–287.